Author/s:
Blauth, C;Mulvaney, P;Hirai, T

Title:
Ligand memory effect in purple quantum dot LEDs

Date:
2019-10-22

Citation:
Blauth, C., Mulvaney, P. & Hirai, T. (2019). Ligand memory effect in purple quantum dot LEDs. Applied Physics Letters, 115 (17), https://doi.org/10.1063/1.5123635.

Persistent Link:
https://hdl.handle.net/11343/368937

RESEARCH ARTICLE | OCTOBER 22 2019

Ligand memory effect in purple quantum dot LEDs

Christian Blauth ; Paul Mulvaney ; Tadahiko Hirai

Appl. Phys. Lett. 115, 173505 (2019)
https://doi.org/10.1063/1.5123635

Applied Physics Letters ARTICLE scitation.org/journal/apl

Ligand memory effect in purple quantum dot LEDs

Cite as: Appl. Phys. Lett. **115**, 173505 (2019); doi: 10.1063/1.5123635
Submitted: 7 August 2019 · Accepted: 9 October 2019 ·
Published Online: 22 October 2019

Christian Blauth,[1,2] Paul Mulvaney,[1] and Tadahiko Hirai[2,a)]

AFFILIATIONS

[1]ARC Centre of Excellence in Exciton Science, School of Chemistry, University of Melbourne, Parkville, Victoria 3010, Australia
[2]CSIRO Manufacturing, Bayview Avenue, Clayton, Victoria 3168, Australia

[a)]Electronic mail: tadahiko.hirai@csiro.au

ABSTRACT

We report a ligand-dependent, trap state memory effect in a purple quantum dot light emitting diode. The measured, bistable current-voltage characteristics show a high conductance state and a low conductance state. Thereby, a memory window with an ON state and an OFF state is achieved, which can be reversed by applying a negative bias. The height of the memory window depends strongly on the length of the ligand passivating the quantum dot (QD). Together with a 5 nm thick aluminum film under the hole transport layer, charges accumulate at the charge transport/quantum dot ligand interface, leading to an increase in conductance during the forward voltage sweep. During a reverse voltage sweep, previously injected charge carriers recombine until the active layer is free of charge carriers. Voltage-capacitance measurements confirm the changes in the charge carrier population within the active layer and demonstrate that they depend on both the direction of the bias sweep and ligands surrounding the QD.

Due to their highly tunable bandgap and their size-dependent electronic and optical characteristics, colloidal quantum dots (QDs) have garnered a lot of attention as potential light emissive layers in next-generation optoelectronic devices, with applications ranging from light emitting diodes (LEDs) in displays, photovoltaic devices, and transistor applications to light emitting transistors that combine switching with light emission.[1–5] However, relatively little research has been performed on the memory functionality of nanomaterials.[6–8] In general, organic/metal/organic device architectures have been used to achieve memory effects in optoelectronic devices, with holes typically being the dominant charge type for the memory effect.[9–11] In 2004, Kang *et al.*[11] reported a memory effect in a layered organic light emitting diode where either a thin silver layer or an organic heterojunction controllably traps and releases electrical charges. A light emitting diode with gold nanoparticles incorporated into the polymer bistable electron transport layer was introduced, which enabled the authors to demonstrate that electrons can be the dominant charge type leading to the memory effect.[12] Depending on the device architecture, electrons or holes can be trapped and thereby create either a low or high conductivity state.

An adjustable memory effect based on the position of particles within the charge transport layer has also been demonstrated through the introduction of silver nanoparticles into a pentacene layer.[13] A layer-by-layer architecture with a polyelectrolyte (PE) ligand/gold nanoparticle was shown to have a flash memory functionality. The memory window itself was controlled by the thickness of the tunneling oxide layer, as well as by the charge trapping mechanism of the ligand/gold nanoparticle interface.[14] Li *et al.*[7] have presented a nonvolatile, bistable memory device where CdSe/ZnS quantum dots were sandwiched between two C_{60} layers. Furthermore, QDs have been embedded into the hole transport layer of an organic bistable LED and this device exhibited bistability under negative bias and light emission under positive bias.[15]

In this report, we incorporate purple quantum dots (QDs), Fig. S1, capped with various ligands of different lengths and electrical conductivities into a standard quantum dot light emitting diode (QLED) architecture where the hole transport layer consists of an organic/metal/organic layer. We report the trapping of charges on the ligands and a ligand-dependent memory effect. We find that the devices fabricated from QDs capped with either longer ligands or less conductive ligands exhibit a large memory window, whereas QDs capped with shorter ligands show limited memory functionality. A full read-write-erase cycle is also demonstrated using capacitance measurements. A simple model explains the formation of the memory window.

The QDs were synthesized following a protocol developed by Bae *et al.*[16] A detailed synthetic route as well as the ligand exchange

procedure has been reported before[17] and are described in the supplementary material.

The QLEDs in this study were prepared in a clean room environment and designed in a sandwich architecture based on patterned 150 nm thick indium tin oxide (ITO) coated glass substrates as the anode. The substrates were cleaned in an ultrasonicator with ethanol and water. 40 nm of N,N′-bis(naphthalen-1-yl)-N,N′-bis(phenyl)-2,2′-dimethylbenzidine (NPD) and a 5 nm thick Al layer were deposited by thermal evaporation. A 50 nm thick poly(9-vinylcarbazole) (PVK) film was cast from a 10 mg/ml chlorobenzene solution and annealed for 30 min at 180 °C. The samples were then transferred into a nitrogen filled glovebox. A 25 nm QD film was deposited from a 20 mg/ml toluene solution by spin coating and dried at 120 °C for 20 min. A 25 nm thick layer of 3,3′,5,5′-tetra[(m-pyridyl)-phen-3-yl]biphenyl (BP4mPy) was thermally deposited as the electron transport layer followed by a LiF/Al (1 nm/100 nm) electrode as the cathode.

Figure 1 shows the I-V characteristics of the QLEDs capped with various amines. The starting voltage for the sweep was always 0 V. A variation in the starting voltage or the preswipe charging time had very little impact on the memory functionality of the devices, suggesting that trap states are filled both quickly and spontaneously. To underline the importance of the Al interlayer and to prove that the effects are truly ligand-based, two control experiments were performed with the same device architecture: first, the Al interlayer was omitted and a device with triphenylamine capped QD was measured. In a second experiment, a device without QDs was tested. By omitting the Al interlayer, the device operates like a standard QLED and does not show a memory window. A change in the sweep direction has little impact on the I-V characteristics. We conclude therefore that the Al interlayer is fundamental for the memory effect.

For all amines, including the control device, we found that a current spike was achieved at 2.5 V during the forward sweep, which creates a high current ON state. At around 4 V, the current overshoot decreased, thereby closing the memory functionality. With increasing bias, a higher current turned the device on. As the memory functionality occurs at a voltage below the device turn-on voltage, no luminescence was observed despite the current density being high enough for luminescent recombination. A low conductance, OFF state, is achieved when the voltage was swept from high to low bias. The difference between the ON and OFF states, as well as the height of the memory window, depends on the ligand surrounding the QDs; short ligands like butylamine show a narrow memory window (0.1 μA), comparable to the control device, whereas their longer counterparts, such as oleylamine or triphenylamine, show an up to 50-fold increase in the memory window with 3.7 μA and 5.6 μA. Despite the fact that the ligands surrounding the QDs change the conductivity of the active layer considerably, the memory window appears at a similar bias for all five ligands.

Figure 2 shows the operating mechanism of the memory effect in a QLED. When the device is driven under forward bias, holes are injected into the NPD/Al interface where they accumulate and build up a memory window, independent of the ligand in the active layer.

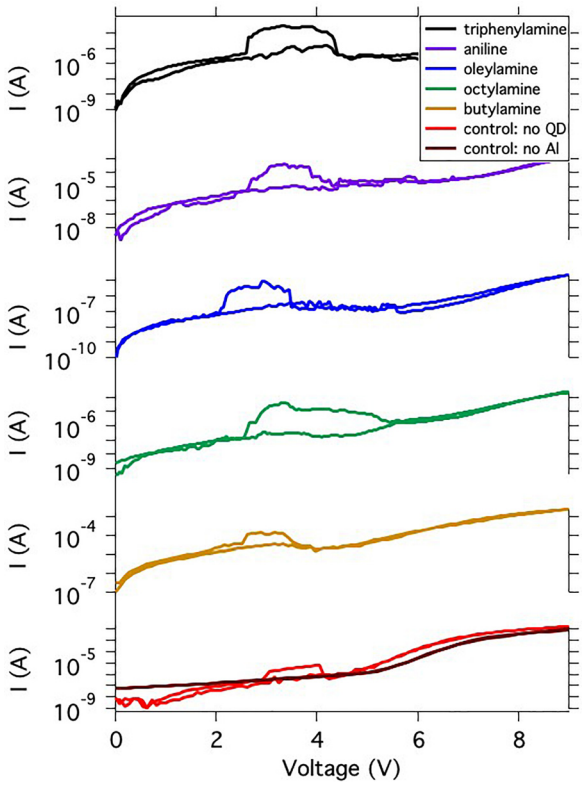

FIG. 1. Current-voltage characteristics of the five amines under test, as well as a control device with the voltage sweep starting at 0 V.

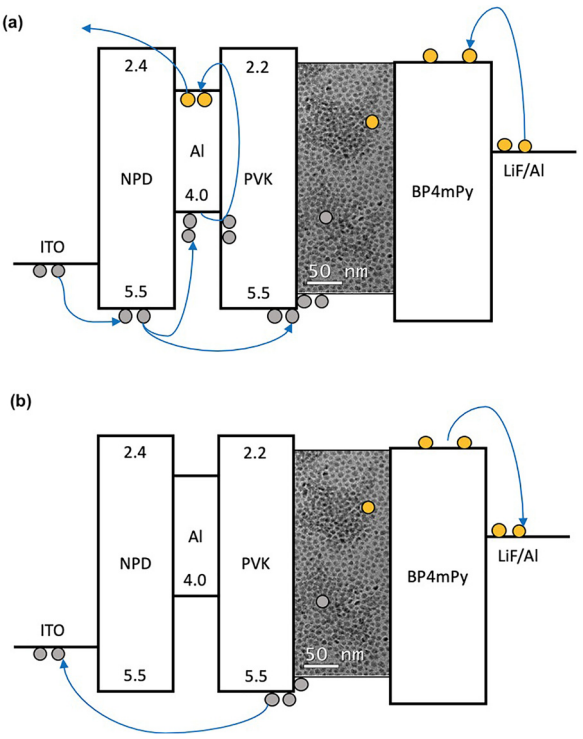

FIG. 2. Operational principle of the memory effect under forward (a) and reversed bias (b).

Bozano *et al.*[18] and Ma *et al.*[8] have shown that thin metal films (<10 nm) on an organic layer cause a discontinuous, clusterlike structure that is thin enough for charges to tunnel through. Electronically, these clusters can be described as an assembly of quantum wells close to each other. Due to the large bandgap of the organic charge transport layers surrounding this Al cluster, electrons tunnel through the barrier, against the direction of the applied electric field, and polarize the Al interlayer, with the charge stored.[8] When the bias is further increased, holes are injected into the PVK and transported to the quantum dot. At the interface, between the PVK and the ligand, charges are trapped again and finally open the ligand-dependent memory window.[17] Because we see a small memory effect with the Al interlayer without QDs, but not when the Al interlayer is left out, we conclude that the Al layer is a prerequisite for the memory effect. Since the type of ligand strongly impacts the height of the memory window, we conclude that the charge trapping at the PVK-ligand interface is dominant. The larger the ligand, the more likely it is for the charges to be trapped and accumulated at the ligand/QD interface, which in turn leads to a larger memory window. More charges are injected into the device with an increased bias, overcoming the trapping and allowing holes and electrons to recombine and for the device to turn on.

Under reverse bias, the amount of injected charge decreases. Charges at the interface close to the electrodes return to their metal contacts and those in the active layer recombine, making the active layer resistive. While recombining, an electric field builds up, which releases charges from shallow trap states and empties the active layer.

The change in the population of charge carriers was confirmed through voltage-capacitance measurements, Fig. 3. In order to approach the DC operating conditions of a QLED, the capacitance measurements were performed at 0.1 Hz. For the purpose of this study, the QLED was modeled as a plate capacitor with the ligand/quantum dot interface defining the active layer. When charges accumulate during increased bias, the active layer is large due to holes and electrons being physically separated, resulting in a rather small capacitance.[19] At 3 V forward sweep, the current increases and opens the memory window, while the capacitance remains low. We can therefore conclude that charges accumulate at the NPD/Al interface and broaden the active layer. With more charges being injected, the capacitance increases and finally turns the device on. When the bias is decreased, the capacitance decreases until approximately 4 V. At this bias, the majority of charges have recombined and the active layer becomes more resistive. Between 4 V and 3 V, the capacitance increases strongly, suggesting that deep trapped charge carriers are released, which makes the active layer highly conductive. Again, at this voltage, a memory window is observed. When the bias is further decreased, the freshly released charges are transported to their electrodes, resulting in the device turning off. Because the control device without QDs shows almost no change between forward and backward sweep, we conclude that the ligands trap charges and the Al interlayer does not impact charges during the reverse sweep.

The ligands surrounding the QDs change the resistance of the active layer, which causes a build-up in capacitance. With the exception of butylamine, all ligands showed a strong increase in capacitance when the bias was decreased. The different behavior of the butylamine

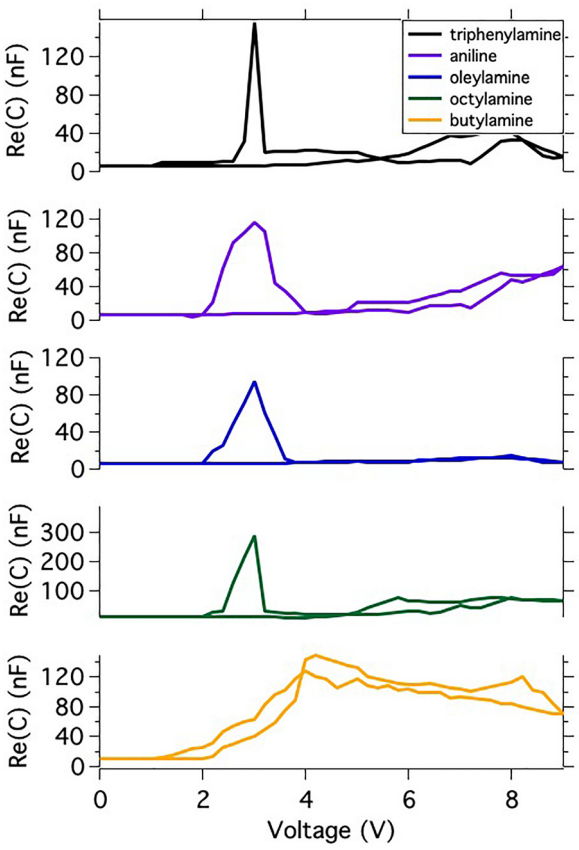

FIG. 3. C-V measurements for the QLEDs with the memory functionality.

capped QLEDs can be explained by the much shorter ligand length and its reduced capability to accumulate and trap charges on the ligand. As Fig. 1 shows, butylamine has the smallest memory window and proportionally the smallest change in capacitance. The larger the memory window in the I-V curves, the larger the accumulation and the storage of charge carriers and hence the bigger the capacitance change on the reverse voltage sweep.

Figure 4(a) shows the I-V characteristics of two memory cycles for devices with each of the five amines used in this study. The different read and reread currents at a bias of 3 V are presented, and Fig. 4(b) shows a stability test.

The memory window remains stable for more than 20 cycles for all amines. After the operation of over 25 memory cycles, in particular, for the butylamine case, additional trap states appear, and these require larger erase voltages to reset the memory functionality. The QLEDs with electrically conductive ligands, such as triphenylamine and particularly aniline, are stable over 500 cycles. QLEDs fabricated from QDs with the electrically insulating ligands, octylamine and oleylamine, retained their memory functionality for more than 400 cycles. The stability of the memory effect is further shown by measuring the retention time, Fig. S2. This is easily achieved by delaying the discharge time before applying a positive reading bias. A bias of +3 V was applied every 10 s. Butylamine-capped QDs showed a current spike for up to two hours, whereas the aniline- and triphenylamine-

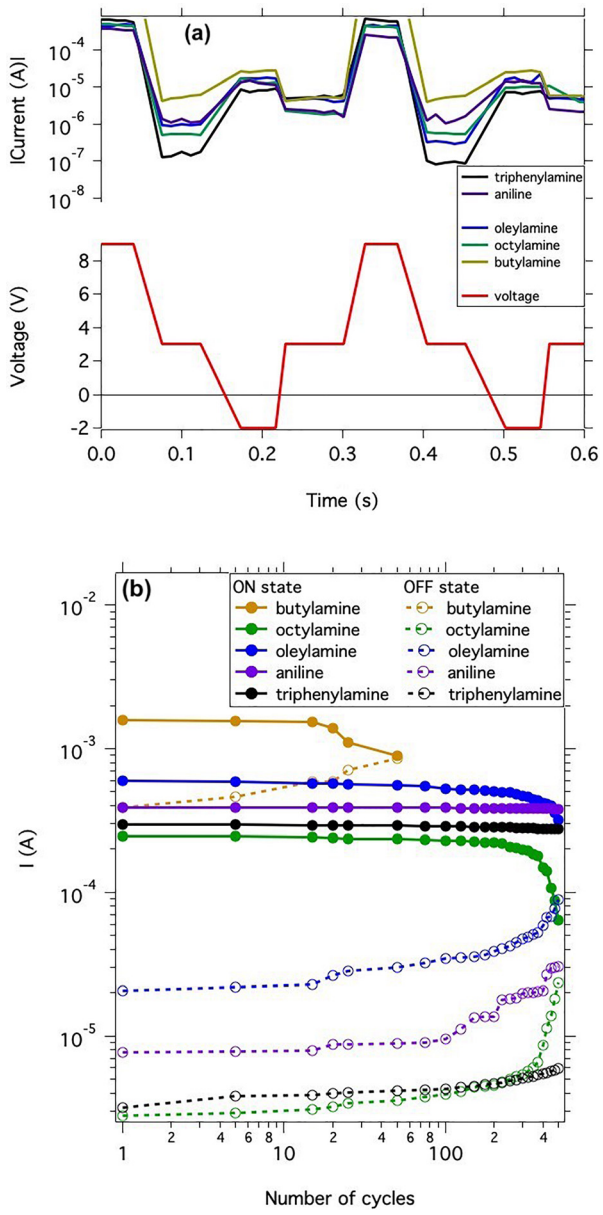

FIG. 4. Memory effect: driving conditions (a) and stability test (b). (a) Memory functionality of all five ligands showing a write-read-erase-reread cycle. The voltages for writing, reading, erasing are 9 V, 3 V, and −2 V, respectively. (b) Stability test for the various QLEDs.

capped QLEDs showed a memory window even after 8 h. The electrically insulating amines retained their charge storage capability for up to 6 h. Currently, the QLEDs with a memory functionality are not stable enough for a commercial application; however, hybrid devices that combine light emission and the storage of charges could be a valuable asset for future electronics. More electrically stable ligands, potentially inorganic ones, could enhance the lifetime of the memory window.

In conclusion, ligands surrounding QDs can store and trap charges, creating a memory window in QLEDs. A metal film together with a charge transport/QD interface can trap and accumulate charges. All ligands show memory functionality. However, the ligand length and electrical conductivity alter the resistivity of the active layer, the charge injection properties, and thereby the height of the memory window. QDs with short ligands show a narrow window (0.1 μA), whereas longer ligands and more electrically conductive ligands open a big memory window of up to 5 μA. Different accumulation properties lead to a memory effect, which has been proved through capacitance-voltage measurements. A memory cycle, with a write-read-erase-reread functionality, is established for all QLEDs, with short ligands showing limited stability and their longer counterparts demonstrating more resilient and repetitive storage and release of charge carriers.

See the supplementary material for a detailed description of the QD synthesis and spectroscopic characterization of the QDs after ligand exchange as well as spectral emission data of the QLEDs.

The authors thank the ARC for support through Grant No. CE170100026 and Anthony Chesman for valuable discussions.

REFERENCES

[1]H. Moon, C. Lee, W. Lee, J. Kim, and H. Chae, Adv. Mater. **31**, 1804294 (2019).
[2]J. Kwak, W. K. Bae, M. Zorn, H. Woo, H. Yoon, J. Lim, S. W. Kang, S. Weber, H.-J. Butt, R. Zentel *et al.*, Adv. Mater. **21**, 5022 (2009).
[3]Y.-L. Lee and Y.-S. Lo, Adv. Funct. Mater. **19**, 604 (2009).
[4]J. Schornbaum, Y. Zakharko, M. Held, S. Thiemann, F. Gannott, and J. Zaumseil, Nano Lett. **15**, 1822 (2015).
[5]Y. Chen, Y. Chu, X. Wu, W. Ou-Yang, and J. Huang, Adv. Mater. **29**, 1704062 (2017).
[6]L. Ma and J. Liu, Appl. Phys. Lett. **80**, 2997 (2002).
[7]F. Li, D.-I. Son, J.-H. Ham, B.-J. Kim, J. H. Jung, and T. W. Kim, Appl. Phys. Lett. **91**, 162109 (2007).
[8]L. Ma, S. Pyo, J. Ouyang, Q. Xu, and Y. Yang, Appl. Phys. Lett. **82**, 1419 (2003).
[9]S. H. Kim, K. S. Yook, J. Y. Lee, and J. Jang, Appl. Phys. Lett. **93**, 053306 (2008).
[10]Y. Yang, J. Ouyang, L. Ma, R.-H. Tseng, and C.-W. Chu, Adv. Funct. Mater. **16**, 1001 (2006).
[11]S. H. Kang, T. Crisp, I. Kymissis, and V. Bulović, Appl. Phys. Lett. **85**, 4666 (2004).
[12]R. J. Tseng, J. Ouyang, C.-W. Chu, J. Huang, and Y. Yang, Appl. Phys. Lett. **88**, 123506 (2006).
[13]S. Wang, C.-W. Leung, and P. K. Chan, Org. Electron. **11**, 990 (2010).
[14]J.-S. Lee, J. Cho, C. Lee, I. Kim, J. Park, Y.-M. Kim, H. Shin, J. Lee, and F. Caruso, Nat. Nanotechnol. **2**, 790 (2007).
[15]S. O. Jeon, K. S. Yook, and J. Y. Lee, Synth. Met. **160**, 1216 (2010).
[16]W. K. Bae, M. K. Nam, K. Char, and S. Lee, Chem. Mater. **20**, 5307 (2008).
[17]C. Blauth, P. Mulvaney, and T. Hirai, J. Appl. Phys. **126**, 075501 (2019).
[18]L. Bozano, B. Kean, V. Deline, J. Salem, and J. Scott, Appl. Phys. Lett. **84**, 607 (2004).
[19]S. Berleb, W. Brütting, and G. Paasch, Org. Electron. **1**, 41 (2000).